Research Square

Preprints are preliminary reports that have not undergone peer review.
They should not be considered conclusive, used to inform clinical practice,
or referenced by the media as validated information.

Three-Dimensional P- and S-Wave Local Earthquake Tomography of the Eastern Alborz, Northern Iran

MohammadReza Sepahvand

sepah55@gmail.com

Graduate University of Advanced Technology

Majid Nemati

Shahid Bahonar University of Kerman

Afsaneh Nasrabadi

Graduate University of Advanced Technology

Zahra Razazi

Graduate University of Advanced Technology

Research Article

Keywords: Local earthquake tomography, Eastern Alborz, Seismicvelocity structure, Seismotectonics

Posted Date: August 1st, 2026

DOI: https://doi.org/10.21203/rs.3.rs-10450921/v1

License: This work is licensed under a Creative Commons Attribution 4.0 International License.
Read Full License

Additional Declarations: No competing interests reported.

Abstract

The eastern Alborz is one of the most tectonically active regions of northern Iran, yet its crustal structure remains poorly constrained. Local earthquake tomography was performed using P- and S-wave travel-time data recorded by temporary and permanent seismic networks between 2007 and 2008. Following quality control, 2,048 local earthquakes recorded by 32 seismic stations were selected for the simultaneous inversion of earthquake hypocenters and seismic velocities with the LOTOS algorithm. Resolution tests indicate that the final models reliably recover the major velocity anomalies within the well-sampled parts of the crust. The resulting Vp, Vs, and Vp/Vs models reveal pronounced lateral heterogeneity and crustal segmentation. Extensive low-velocity anomalies spatially coincide with the principal active fault systems and relocated seismicity, indicating that active deformation is preferentially localized within mechanically heterogeneous crustal domains. The models also reveal two previously unrecognized low-velocity lineaments in the southeastern part of the study area, suggesting the presence of concealed fault-related structures. A persistent low-velocity anomaly associated with relatively elevated Vp/Vs values is also observed beneath the Damavand volcanic center. These results provide a seismic velocity model of the eastern Alborz and offer new constraints on crustal segmentation, concealed fault-related structures, and the relationship between seismic velocity heterogeneity and active deformation. They also provide an improved geophysical framework for understanding active tectonics and assessing seismic hazard within the northern sector of the Arabia–Eurasia collision zone.

Highlights

Seismic imaging reveals strong crustal heterogeneity beneath the eastern Alborz.

Low-velocity zones spatially correlate with active fault systems and seismicity.

Previously unrecognized low-velocity lineaments suggest concealed fault-related structures.

1 Introduction

Iran is situated within one of the most tectonically active sectors of the Alpine–Himalayan orogenic belt, where the ongoing convergence between the Arabian and Eurasian plates controls the present-day deformation of the region. This convergence has generated widespread crustal shortening, active faulting, and distributed intracontinental deformation, leading to the development of the Zagros and Alborz mountain belts (McKenzie, 1972; Jackson and McKenzie, 1984; Allen et al., 2004; Mouthereau et al., 2012). Geodetic observations indicate convergence rates of approximately 20–25 mm yr^{-1}, accommodated through a combination of thrust faulting, strike-slip faulting, and distributed crustal shortening (Vernant et al., 2004; Masson et al., 2007; Walpersdorf et al., 2014). Consequently, northern Iran is characterized by persistent seismic activity and represents one of the most seismically hazardous regions of the Arabia–Eurasia collision zone.

The Alborz Mountains form a narrow but tectonically active intracontinental orogenic belt separating the Iranian Plateau from the South Caspian Basin. Deformation within the range is highly heterogeneous and is partitioned among several major active fault systems (Berberian and Yeats, 1999; Jackson et al., 2002; Allen et al., 2003). In the eastern Alborz, crustal shortening is mainly accommodated by the Khazar, North Alborz, Mosha, Astaneh, Firuzkuh, Garmsar, and North Semnan fault systems through a combination of reverse and left-lateral strike-slip faulting (Berberian et al., 1992; Nazari et al., 2009; Nemati et al., 2011). A tectonic overview of the study area together with the principal active faults is shown in Fig. 1. Structural trends progressively rotate from northwest–southeast in the western Alborz to northeast–southwest in the eastern sector, reflecting significant crustal segmentation and variations in regional deformation (Allen et al., 2011). Recent structural investigations further indicate that deformation is distributed among multiple interacting fault segments rather than a single continuous fault system, emphasizing the structural complexity of the Alborz belt (Rashidi et al., 2023).

The eastern Alborz is additionally characterized by intense seismicity and the presence of the Quaternary Damavand volcanic system, making it an ideal natural laboratory for investigating the relationship between active faulting, seismicity, and crustal structure. Previous receiver-function studies, regional tomography, and crustal imaging have revealed pronounced lateral variations in crustal thickness and seismic velocity beneath the Alborz Mountains and the South Caspian Basin (Mangino and Priestley, 1998; Sodoudi et al., 2009; Abbassi et al., 2010; Rezaeifar and Kissling, 2020). Although these studies successfully resolved the first-order lithospheric structure of northern Iran, their spatial resolution is insufficient to image fault-scale heterogeneity within the eastern Alborz. In particular, the regional tomography of Rezaeifar and Kissling (2020) identified broad low-velocity anomalies beneath the Alborz, including the Damavand volcanic region, and highlighted the need for higher-resolution local investigations to better resolve shallow crustal structures and their relationship with active tectonics.

Previous investigations in the eastern Alborz have mainly focused on earthquake distribution, fault kinematics, focal mechanisms, and active deformation (Ritz et al., 2006; Nazari et al., 2009; Nemati et al., 2011). Regional seismic tomography and receiver-function studies have further improved the understanding of the crustal and lithospheric structure beneath northern Iran (Alinaghi et al., 2007; Kaviani et al., 2007; Sodoudi et al., 2009; Rezaeifar and Kissling, 2020). Nevertheless, the spatial resolution of these regional models is insufficient to resolve fault-scale velocity heterogeneity within the eastern Alborz, where deformation is distributed among several closely spaced active fault systems. As a result, the three-dimensional geometry, continuity, and depth extent of crustal velocity anomalies associated with these structures remain poorly constrained.

Local earthquake tomography provides an effective means of imaging crustal heterogeneity because P-wave and S-wave velocity variations are sensitive to changes in lithology, fracture density, temperature, and fluid distribution. Moreover, the Vp/Vs ratio provides additional information on crustal elastic properties and has been widely used to distinguish mechanically weak or fluid-rich zones from relatively competent crust. Despite the tectonic importance of the eastern Alborz and the presence of the

Damavand volcanic system, detailed three-dimensional imaging of crustal Vp, Vs, and Vp/Vs variations has remained limited.

To improve understanding of the crustal structure of the eastern Alborz, local earthquake tomography was applied to P- and S-wave arrival-time data recorded by temporary and permanent seismic networks. The resulting velocity models, integrated with relocated seismicity and the distribution of major active faults, provide new constraints on crustal heterogeneity, fault-controlled deformation, concealed structural features, and the seismotectonic evolution of this sector of the Arabia–Eurasia collision zone.

2 Seismic Data

Local microearthquakes used in this study were recorded by two temporary seismic networks deployed by the Geological Survey of Iran and complemented by permanent stations operated by the Institute of Geophysics, University of Tehran (Fig. 2). Seismic monitoring was carried out during 2007–2008, providing broad spatial coverage of the eastern Alborz region.

Part of this dataset was previously used for earthquake relocation, seismotectonic analysis, focal mechanism determination, and the construction of a one-dimensional reference velocity model (Nemati et al., 2011). However, it has not previously been analyzed using local earthquake tomography. In the present study, the archived P- and S-wave arrival-time data were reanalyzed using the LOTOS-12 Release tomography package to derive Vp and Vs velocity models of the eastern Alborz crust.

A total of 32 seismic stations were included in the analysis. Waveforms were manually inspected, and only high-quality P- and S-wave arrivals were retained following standard seismological quality-control criteria. Events with poor azimuthal coverage, insufficient phase readings, or large travel-time residuals were excluded. After quality control, 2,048 local earthquakes with reliable P- and S-wave arrivals were selected for tomographic inversion (Fig. 3). The resulting dataset provides adequate ray-path coverage for the simultaneous inversion of earthquake hypocenters and crustal velocity structure.

3 Methodology

3.1 Tomographic Inversion

Local earthquake tomography simultaneously estimates seismic velocity structure and earthquake hypocenters from observed P- and S-wave travel times. Because travel times depend on both crustal velocity heterogeneity and earthquake locations, simultaneous inversion reduces parameter trade-offs and improves model stability.

The Vp and Vs models were obtained using the LOTOS-12 Release tomography package (Koulakov, 2009), which jointly inverts earthquake locations and seismic velocity structure. An optimal one-dimensional reference model was established through iterative minimization of travel-time residuals and subsequently used as the initial model for the inversion. The starting model was adopted from Nemati et

al. (2011) (Table 1) and further constrained by reduced travel-time analysis (Fig. 4). To improve inversion stability at greater depths, an additional velocity interface was introduced at 35 km, where the P-wave velocity was fixed at 8.01 km s^{-1} following Abbassi et al. (2010).

Several alternative one-dimensional velocity models with different layer configurations and Vp/Vs ratios were evaluated to identify the most stable starting model. The final reference model, characterized by a Vp/Vs ratio of 1.70 (Table 1), yielded the lowest travel-time residuals and the most stable convergence.

Ray paths were calculated using a bending ray-tracing algorithm, and the velocity model was parameterized on an irregular grid with node spacing adapted to the ray distribution. To reduce grid-orientation effects, the inversion was repeated using several rotated grids, and the final model was obtained by averaging the individual solutions. The inverse problem was solved using the LSQR algorithm with damping and smoothing regularization. Prior to inversion, all phase picks were manually verified, converted to the LOTOS input format, and filtered to retain only earthquakes with reliable P- and S-wave arrivals and adequate azimuthal station coverage.

Table 1
Initial one-dimensional P-wave velocity model used for the LOTOS inversion.

Depth (km)	Vp (km/s)	
0.0	5.95	Vp/Vs = 1.70
2.0	6.15	
10.0	6.25	
14.0	6.39	
22.0	6.43	
33.5	8.0	
35.0	8.01	
74.0	8.01	

3.2 Selection of Inversion Parameters

The optimal inversion parameters were determined through 60 synthetic checkerboard tests using different combinations of damping, smoothing, and weighting parameters. The parameter values were progressively adjusted based on the recovery of synthetic anomalies and the corresponding reduction in travel-time residuals. The final parameter set was selected as the best compromise between data fit, model smoothness, and anomaly recovery.

The final inversion employed upper-crust weighting factors of 0.8 for both the P- and S-wave models, smoothing coefficients of 0.9 for Vp and 1.6 for Vs, regularization parameters of 0.6 for Vp and 0.9 for

Vs, and a station-correction weight of 0.006 for both datasets. These parameters yielded stable convergence while preserving the geometry and amplitude of the recovered anomalies. The optimized inversion parameters adopted for the final models are summarized in Table 2.

Table 2
Optimal inversion regularization parameters adopted for the final P- and S-wave tomographic inversion.

Parameter	P-wave (Vp)	S-wave (Vs)
Upper-crust model weighting	0.8	0.8
Smoothing coefficient	0.9	1.6
Regularization level	0.6	0.9
Station-correction weight	0.006	0.006

3.3 Resolution Assessment Using Synthetic Checkerboard Tests

Model resolution was assessed using synthetic checkerboard tests performed with the optimized inversion parameters. The checkerboard model consisted of alternating positive and negative velocity anomalies measuring 35 × 35 km, separated by 10-km gaps. Velocity perturbations of ± 10% relative to the initial one-dimensional reference model were assigned to both the Vp and Vs models.

Synthetic travel times were calculated using the actual source–receiver geometry, and random Gaussian noise was added to simulate picking uncertainties. Root-mean-square noise levels of 0.15 s for P-wave arrivals and 0.30 s for S-wave arrivals were applied.

Checkerboard recovery was evaluated at depths of 5, 15, 25, 35, and 40 km for both the Vp and Vs models (Figs. 5 and 6). The recovered patterns show good reconstruction of the imposed anomalies within the central part of the study area, where ray-path coverage is densest. Resolution progressively decreases toward the model margins and at greater depths because of reduced ray coverage. Although anomaly amplitudes are partially attenuated in these regions, their geometry and polarity remain well preserved within the well-resolved areas. These results demonstrate that the selected inversion parameters provide an appropriate balance between data fit, model smoothness, and anomaly recovery, supporting the reliability of the final tomographic models. Accordingly, the geological interpretations presented in this study are restricted to the well-resolved portions of the models.

4 Results

The Vp and Vs models derived from local earthquake tomography reveal pronounced lateral heterogeneity throughout the crust of the eastern Alborz (Fig. 7). Figure 7 presents horizontal slices through both velocity models. Resolution is highest within the upper and middle crust, where earthquake

density and ray-path coverage are greatest, and gradually decreases toward the model margins and at greater depth.

The tomographic images display significant velocity variations at depths of 5, 10, 15, 20, and 25 km. Extensive low-velocity anomalies form elongated NE–SW-trending patterns broadly parallel to the regional tectonic grain. These anomalies are consistently observed in both the Vp and Vs models, persist through successive depth slices, and spatially coincide with relocated seismicity and the major active fault systems, including the North Alborz, Astaneh, and North Semnan faults.

Two prominent low-velocity lineaments (F1 and F2) are identified in the southeastern part of the study area near the mountain–plain transition zone (Fig. 7). These features remain continuous through several depth slices and locally differ in orientation from previously mapped surface structures. Their possible tectonic significance is discussed below.

A persistent low-velocity anomaly is also imaged beneath the Damavand volcanic center, extending from the shallow crust to depths of at least 25 km. In contrast, relatively high-velocity bodies occur as isolated domains adjacent to the low-velocity regions and generally coincide with areas of lower seismicity.

The three-dimensional Vp/Vs model (Fig. 8) complements the velocity models by revealing marked variations in crustal elastic properties. Elevated Vp/Vs values occur mainly within the central and southwestern parts of the study area and consistently coincide with the principal low-velocity anomalies and the highest density of relocated earthquakes. At greater depths, these anomalies remain laterally continuous but become progressively more localized, whereas lower Vp/Vs values are generally associated with relatively high-velocity domains.

Overall, the Vp, Vs, and Vp/Vs models exhibit a high degree of spatial consistency. Low-velocity regions are generally associated with elevated Vp/Vs values, major fault systems, and concentrated seismicity, whereas high-velocity domains commonly display lower Vp/Vs ratios. These observations indicate that the crust beneath the eastern Alborz is strongly heterogeneous and structurally segmented.

5 Discussion

Previous investigations in the eastern Alborz have primarily focused on earthquake distribution, fault kinematics, and one-dimensional velocity modeling (Nemati et al., 2011). In contrast, this study presents a 3D local earthquake tomography model of the eastern Alborz, providing new constraints on the spatial distribution of Vp, Vs, and Vp/Vs within the crust. Combined with relocated seismicity, these models provide a more comprehensive view of crustal architecture than can be obtained from earthquake locations or focal mechanisms alone.

The tomographic models reveal that the crust beneath the eastern Alborz is highly heterogeneous and laterally segmented. Low-velocity anomalies are consistently observed in both the Vp and Vs models, where they spatially coincide with the principal tectonic trends and clusters of relocated earthquakes.

Their persistence through successive depth levels indicates that these anomalies represent deep-rooted crustal heterogeneity rather than isolated shallow features. These observations are consistent with previous seismic tomography studies in northern Iran, including the regional lithospheric model of Alinaghi et al. (2007) and the higher-resolution crustal model of Rezaeifar and Kissling (2020), both of which documented pronounced seismic velocity heterogeneity beneath the Alborz Mountains. Owing to the denser local earthquake dataset used in the present study, however, the eastern Alborz is resolved at considerably higher spatial resolution, allowing smaller-scale structural features to be identified.

A close spatial correspondence is observed between the velocity anomalies and the major active fault systems, including the North Alborz, Astaneh, and North Semnan faults. Earthquake clusters are preferentially concentrated within or adjacent to the low-velocity domains. Because earthquake relocation and velocity inversion were performed simultaneously using the LOTOS algorithm, this relationship is unlikely to result solely from relocation bias and instead reflects the structural control exerted by the active fault network. Similar spatial associations between crustal velocity heterogeneity and active fault systems have also been reported from the Central Alborz by Afra et al. (2021), suggesting that mechanically heterogeneous crust represents a characteristic feature of deformation throughout the Alborz belt rather than being restricted to its central sector.

One of the principal findings of this study is the identification of two coherent low-velocity lineaments (F1 and F2) in the southeastern part of the study area. These features persist through several depth slices but do not completely coincide with previously mapped surface faults, suggesting the presence of buried or previously unrecognized fault-related structures beneath the mountain–plain transition zone. Such structures were not resolved in previous regional tomographic studies, highlighting the improved imaging capability achieved by the dense local earthquake dataset used here. Nevertheless, their geometry and kinematic significance cannot be fully constrained by the present tomography alone and require confirmation through complementary geological and geophysical investigations.

The Vp/Vs model provides an important complement to the individual velocity models. Elevated Vp/Vs values consistently coincide with low-velocity regions and concentrated seismicity, whereas lower ratios generally correspond to relatively high-velocity domains. These systematic spatial relationships indicate substantial variations in crustal physical properties, including fracture density, lithological heterogeneity, and possibly interconnected crustal fluids. The overall distribution of the Vp/Vs anomalies is compatible with recent seismic imaging studies in northern Iran (Rezaeifar and Kissling, 2020; Afra et al., 2021), which similarly emphasize the influence of crustal heterogeneity on active deformation.

A persistent low-velocity anomaly is also imaged beneath the Damavand volcanic center, where reduced Vp and Vs values are accompanied by relatively elevated Vp/Vs ratios. This observation agrees with recent integrated geophysical and petrological modelling of the Damavand volcanic system (Mousavi et al., 2023), which suggests that the crust beneath the volcano is characterized by significant thermal and compositional heterogeneity. Although seismic tomography alone cannot uniquely distinguish among elevated temperature, hydrothermal alteration, partial melt, or fluid-rich crust, the present results clearly

demonstrate that the physical properties beneath Damavand differ substantially from those of the surrounding crust.

Overall, the combined interpretation of the Vp, Vs, and Vp/Vs models indicates that deformation within the eastern Alborz is preferentially localized within laterally heterogeneous crustal domains associated with the major active fault systems. Beyond confirming the regional-scale heterogeneity reported by previous studies, the present work provides three-dimensional images of the eastern Alborz crust, identifies previously unresolved low-velocity lineaments (F1 and F2), and establishes an improved geophysical framework for investigating crustal segmentation, concealed fault structures, and seismic hazard within the northern sector of the Arabia–Eurasia collision zone.

6 Conclusions

This work presents a local earthquake tomography model of the eastern Alborz, providing images of the crustal P-wave velocity (Vp), S-wave velocity (Vs), and Vp/Vs structure using local earthquake data recorded by temporary and permanent seismic networks. The present model is reliable within the well-resolved portions of the study area. Resolution decreases toward the model boundaries and below approximately 30–35 km owing to reduced ray coverage. Therefore, geological interpretations are restricted to these well-resolved regions.

The tomographic models demonstrate that the crust beneath the eastern Alborz is strongly heterogeneous and structurally segmented. Low-velocity anomalies imaged in both the Vp and Vs models are closely associated with the principal active fault systems and clusters of relocated earthquakes, indicating that contemporary deformation is preferentially localized within mechanically heterogeneous crustal domains.

A major outcome of this work is the identification of two coherent low-velocity lineaments (F1 and F2) in the southeastern part of the study area. Their persistence through multiple depth levels and limited correspondence with previously mapped surface faults suggest the presence of concealed fault-related structures that warrant further geological and geophysical investigation.

The Vp/Vs model provides complementary constraints on crustal physical properties, revealing a systematic spatial association between elevated Vp/Vs values, reduced seismic velocities, and concentrated seismicity. In contrast, relatively high-velocity regions are generally characterized by lower Vp/Vs ratios, emphasizing the close relationship between crustal heterogeneity, active faulting, and present-day deformation.

A persistent low-velocity anomaly beneath the Damavand volcanic center, accompanied by relatively elevated Vp/Vs values, further indicates significant physical heterogeneity beneath the volcanic system. Although seismic tomography alone cannot uniquely determine its origin, these observations provide an important basis for future multidisciplinary investigations integrating seismic, geological, and geodetic data.

Overall, the resulting velocity models provide new constraints on the crustal architecture of the eastern Alborz. Beyond documenting regional crustal heterogeneity, they identify previously unresolved fault-related structures and clarify the relationship between seismic velocity variations, active faulting, and earthquake distribution. These findings establish an improved geophysical framework for future tectonic studies and regional seismic hazard assessment within the northern sector of the Arabia–Eurasia collision zone.

Declarations

The authors declare that they have no known competing financial interests or personal relationships that could have appeared to influence the work reported in this paper.

Competing Interests

The authors declare that they have no known competing financial or non-financial interests that could have appeared to influence the work reported in this paper.

Funding

The authors did not receive support from any organization for the submitted work.

Author Contribution

M.S. supervised and guided the study, contributed to the study conception, interpreted the results, prepared the figures, and wrote the manuscript. M.N. conceived the seismic network and provided the seismic dataset used in this study. A.N. contributed to the study conception, interpretation of the results, and critical revision of the manuscript. Z.R. processed and analyzed the seismic data. All authors reviewed and approved the final manuscript.

Acknowledgement

AcknowledgementsThe authors gratefully acknowledge the Geological Survey of Iran (GSI) for providing the seismic data used in this study.

Data Availability

Data AvailabilityThe seismic data used in this study were provided by the Geological Survey of Iran (GSI) and complemented by data from permanent seismic stations operated by the Institute of Geophysics,

University of Tehran. The data are not publicly available but may be available from the corresponding author upon reasonable request and subject to permission from the data providers.

References

1. Abbassi A, Nasrabadi A, Tatar M, Yaminifard F, Abbassi M, Hatzfeld D, Priestley K (2010) Crustal velocity structure in the southern edge of the Central Alborz (Iran). J Geodyn 49:68–78. https://doi.org/10.1016/j.jog.2009.09.044
2. Afra M, Shirzad T, Farrokhi M, Braunmiller J, Hatami M-R, Naghavi M, Rahimi H, Motavalli-Anbaran S-H, Entezar-Saadat V, Saadat SA (2021) Three-dimensional P-wave tomography in the Central Alborz, Iran. Phys Earth Planet Inter 315:106711. https://doi.org/10.1016/j.pepi.2021.106711
3. Alinaghi A, Koulakov I, Thybo H (2007) Seismic tomographic imaging of the lithosphere beneath the Alborz Mountains, Iran. Geophys J Int 169:1089–1102. https://doi.org/10.1111/j.1365-246X.2007.03314.x
4. Allen MB, Jackson J, Walker R (2004) Late Cenozoic reorganization of the Arabia–Eurasia collision and the comparison of short-term and long-term deformation rates. Tectonics 23:TC2008. https://doi.org/10.1029/2003TC001530
5. Allen MB, Kheirkhah M, Emami MH, Jones SJ (2011) Right-lateral shear across Iran and kinematic change in the Arabia–Eurasia collision zone. Geophys J Int 184:555–574. https://doi.org/10.1111/j.1365-246X.2010.04874.x
6. Allen MB, Vincent SJ, Alsop GI, Ismail-Zadeh A, Flecker R (2003) Late Cenozoic deformation in the South Caspian region: effects of a rigid basement block within a collision zone. Tectonophysics 366:223–239. https://doi.org/10.1016/S0040-1951(03)00098-2
7. Berberian M, Yeats RS (1999) Patterns of historical earthquake rupture in the Iranian Plateau. Bull Seismol Soc Am 89:120–139.
8. Davidson J, Hassanzadeh J, Berzins R, Stockli DF, Bashukooh B, Turrin B, Pandamouz A (2004) The geology of Damavand volcano, Alborz Mountains, northern Iran. Geol Soc Am Bull 116:16–29. https://doi.org/10.1130/B25344.1
9. Djamour Y, Vernant P, Bayer R, Nankali H, Ritz JF, Hinderer J, Hatam Y (2010) GPS and gravity constraints on continental deformation in the Alborz mountain range, Iran. Geophys J Int 183:1287–1301. https://doi.org/10.1111/j.1365-246X.2010.04811.x
10. Jackson J, McKenzie D (1984) Active tectonics of the Alpine–Himalayan Belt between western Turkey and Pakistan. Geophys J R Astron Soc 77:185–264. https://doi.org/10.1111/j.1365-246X.1984.tb01931.x
11. Jackson J, Priestley K, Allen M, Berberian M (2002) Active tectonics of the South Caspian Basin. Geophys J Int 148:214–245. https://doi.org/10.1046/j.1365-246X.2002.01588.x
12. Koulakov I (2009) LOTOS code for local earthquake tomographic inversion: benchmarks for testing tomographic algorithms. Bull Seismol Soc Am 99:194–214. https://doi.org/10.1785/0120080013

13. Masson F, Anvari M, Djamour Y, Walpersdorf A, Tavakoli F, Daignières M, Nankali H, Van Gorp S (2007) Large-scale velocity field and strain tensor in Iran inferred from GPS measurements: New insight for the present-day deformation pattern within NE Iran. *Geophysical Journal International* 170:436–440. https://doi.org/10.1111/j.1365-246X.2007.03477.x
14. McKenzie D (1972) Active tectonics of the Mediterranean region. Geophys J R Astron Soc 30:109–185. https://doi.org/10.1111/j.1365-246X.1972.tb02351.x
15. Mousavi N, Tatar M, Shafaii Moghadam H, Griffin WL (2023) Integrated geophysical-petrological model of Damavand volcano, North Iran: Compositional structure of crust and upper mantle from seismic temperature profiling and gravity anomaly fitting. J Volcanol Geotherm Res 442:107913. https://doi.org/10.1016/j.jvolgeores.2023.107913
16. Mouthereau F, Lacombe O, Vergés J (2012) Building the Zagros collisional orogen: timing, strain distribution and the dynamics of Arabia–Eurasia plate convergence. Tectonophysics 532–535:27–60. https://doi.org/10.1016/j.tecto.2012.01.022
17. Nazari H, Ritz JF, Salamati R, Shafei A, Solaymani S, Vernant P (2009) Paleoseismological investigations along the Mosha fault, central Alborz, Iran. Tectonophysics 476:293–306. https://doi.org/10.1016/j.tecto.2009.02.032
18. Nemati M, Hatzfeld D, Gheitanchi MR, Sadidkhouy A, Mirzaei N (2011) Microseismicity and seismotectonics of the Firuzkuh and Astaneh faults (East Alborz, Iran). Tectonophysics 506:11–21. https://doi.org/10.1016/j.tecto.2011.04.007
19. Rezaeifar M, Kissling E (2020) Regional 3-D lithosphere structure of the northern half of Iran by local earthquake tomography. Geophys J Int 223:1956–1972. https://doi.org/10.1093/gji/ggaa431
20. Ritz JF, Nazari H, Ghassemi A, Salamati R, Shafei A, Solaymani S, Vernant P (2006) Active transtension inside central Alborz: a new insight into northern Iran–southern Caspian geodynamics. Geology 34:477–480. https://doi.org/10.1130/G22319.1
21. Sodoudi F, Yuan X, Kind R, Heit B, Sadidkhouy A (2009) Evidence for a missing crustal root and a thin lithosphere beneath the Central Alborz by receiver function studies. Geophys J Int 177:733–742. https://doi.org/10.1111/j.1365-246X.2008.04073.x
22. Vernant P, Nilforoushan F, Hatzfeld D, Abbassi M, Vigny C, Masson F, Nankali H, Martinod J, Ashtiani A, Bayer R, Tavakoli F, Chéry J (2004) Present-day crustal deformation and plate kinematics in the Middle East constrained by GPS measurements in Iran and northern Oman. Geophys J Int 157:381–398. https://doi.org/10.1111/j.1365-246X.2004.02222.x
23. Walpersdorf A, Manighetti I, Mousavi Z, Tavakoli F, Vergnolle M, Jadidi A, Hatzfeld D (2014) Present-day kinematics and fault slip rates in eastern Iran derived from GPS measurements. Geophys J Int 198:1163–1184. https://doi.org/10.1093/gji/ggu141

Figures

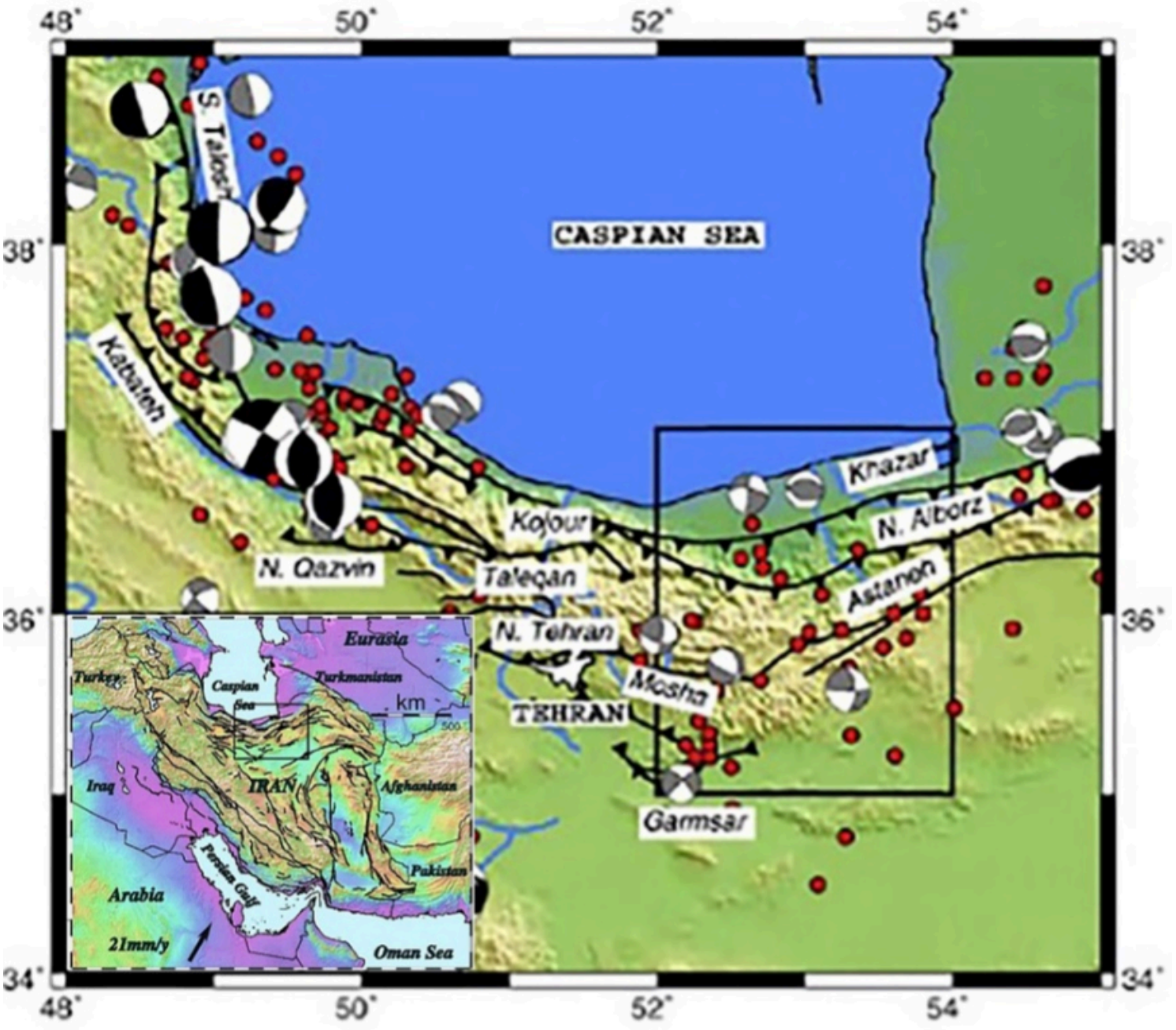


Figure 1

Tectonic map of the Alborz region. The study area is outlined by a rectangle. Red circles indicate earthquakes with magnitudes mb ≥ 4.5, compiled from Nemati et al. (2011).

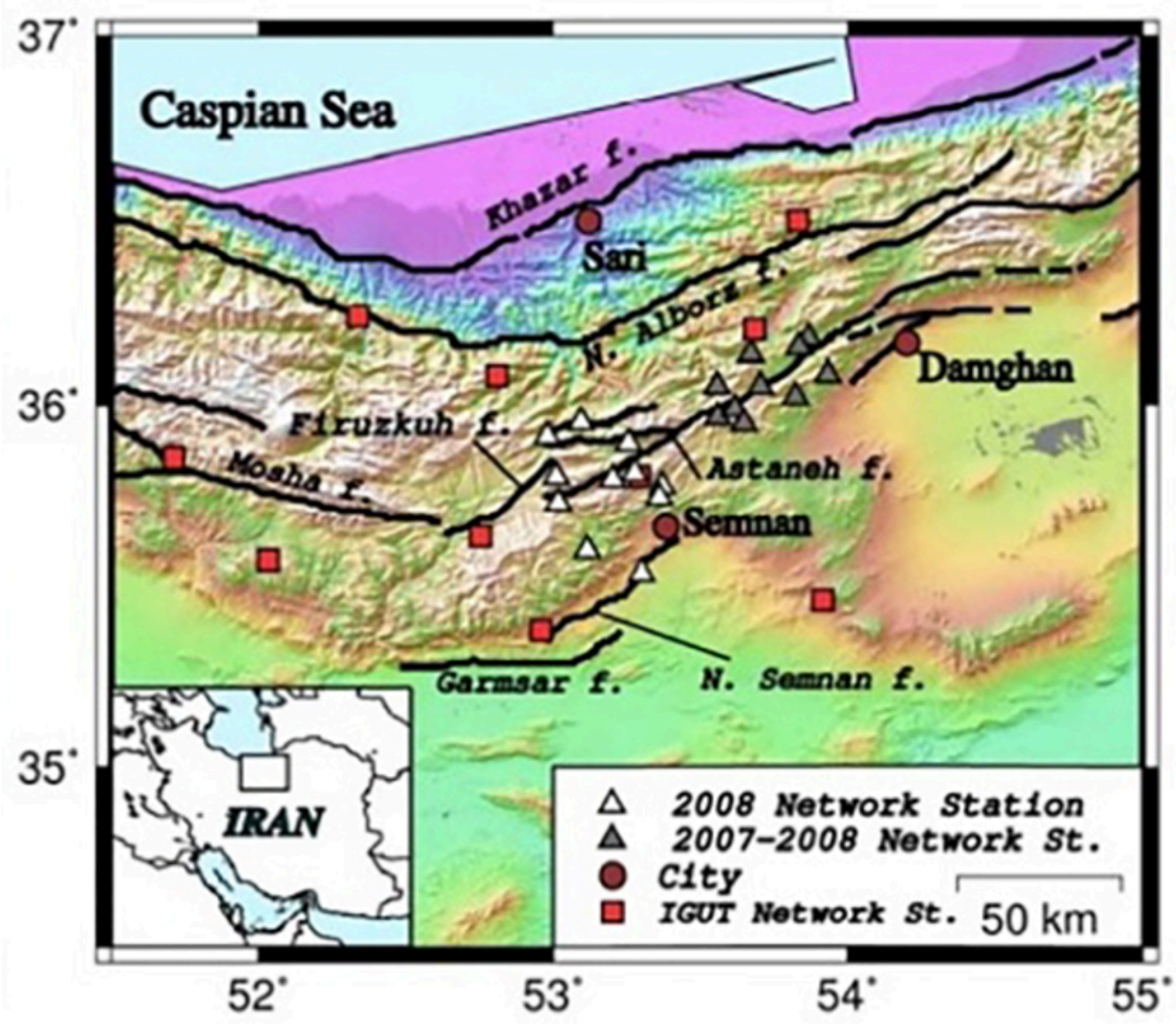


Figure 2

Configuration of the seismic stations in the study area, including the temporary seismic networks (dark and light triangles) and the permanent network of the Institute of Geophysics, University of Tehran (red squares), together with the locations of cities and mapped faults.

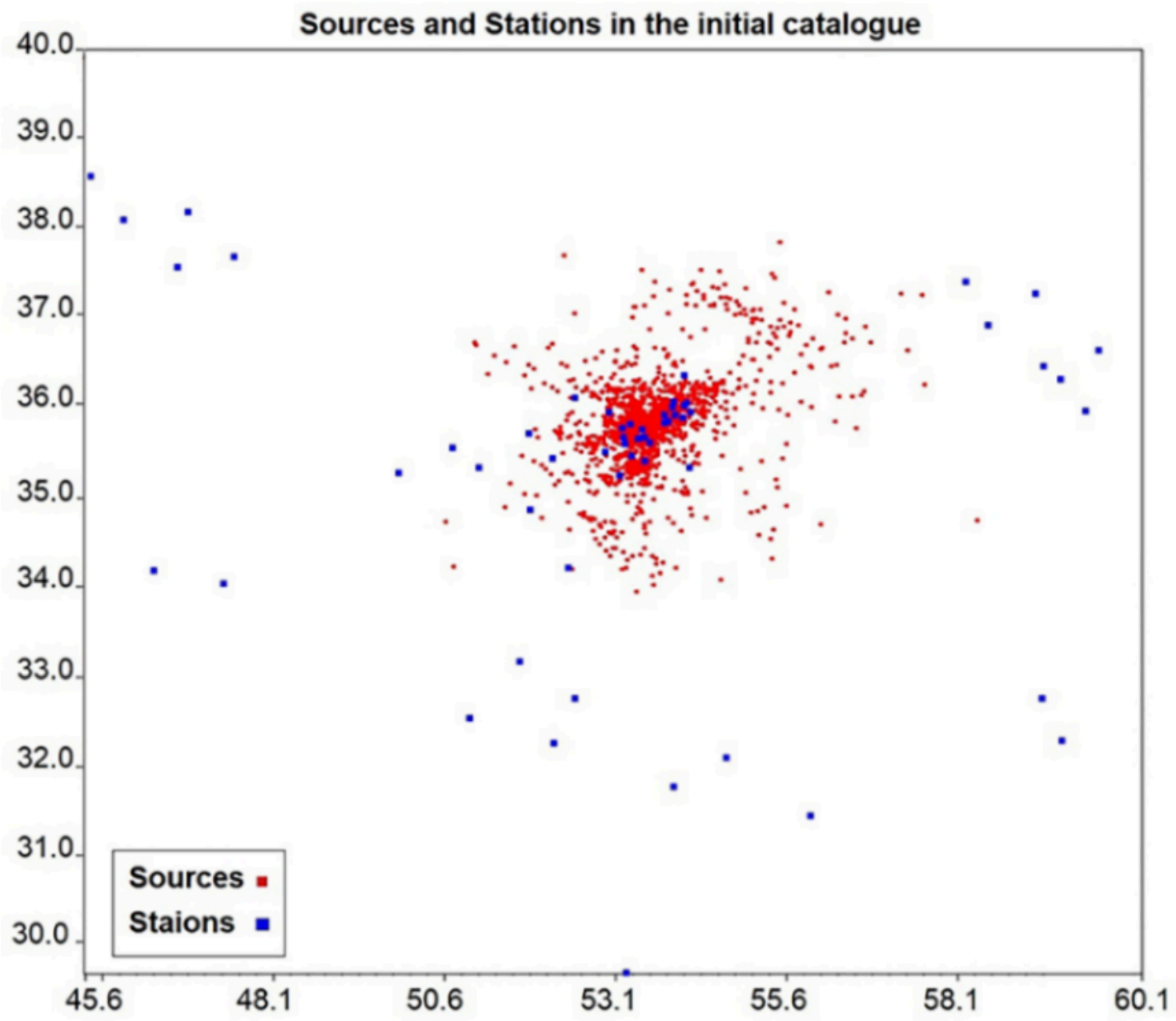


Figure 3

Number of 2048 earthquakes (red dots) recorded with 32 local and regional stations (blue rectangles). Outlier earthquakes with far distances were omitted.

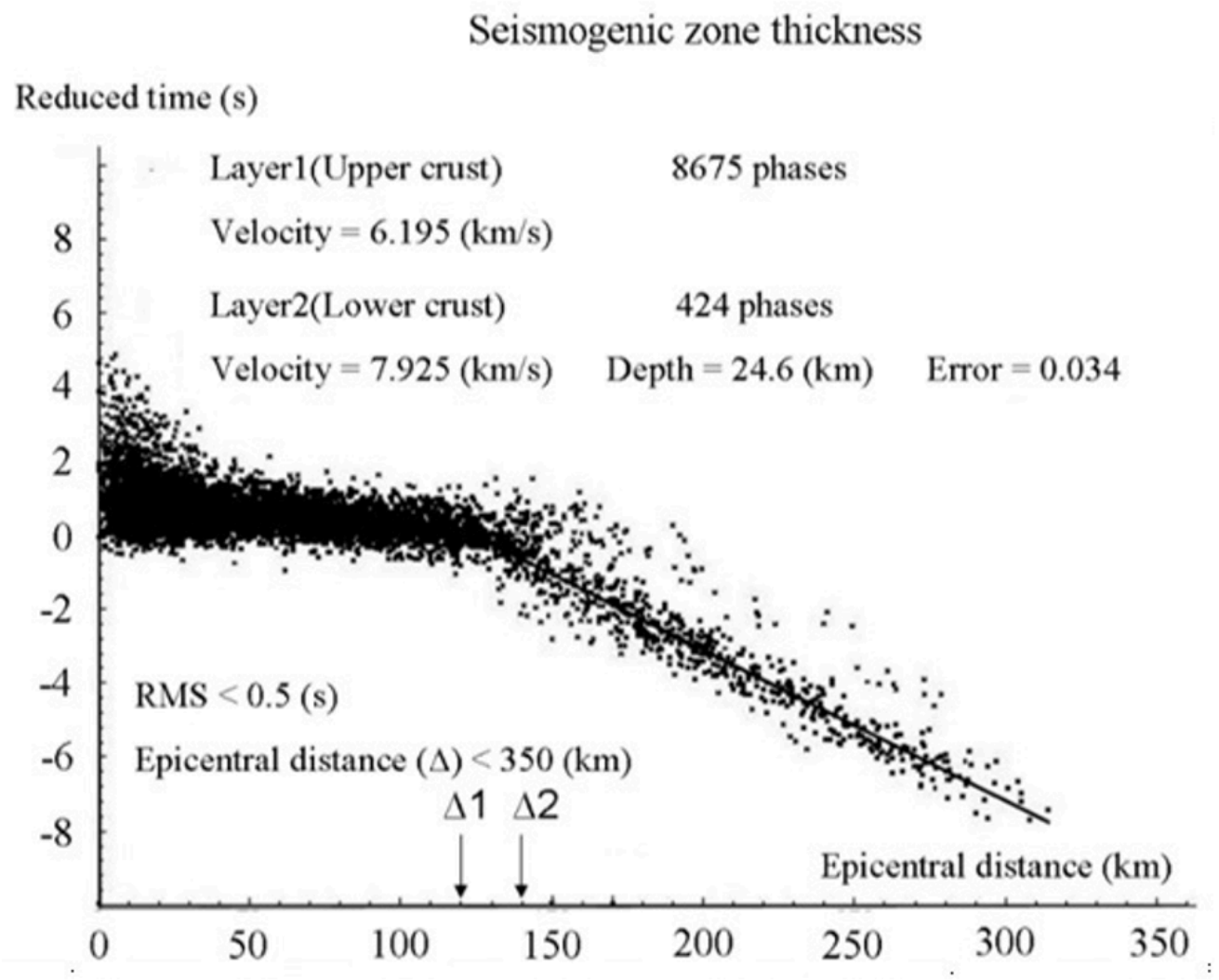


Figure 4

Determination of the Conrad discontinuity from one-dimensional local earthquake tomography using local and regional seismic events.

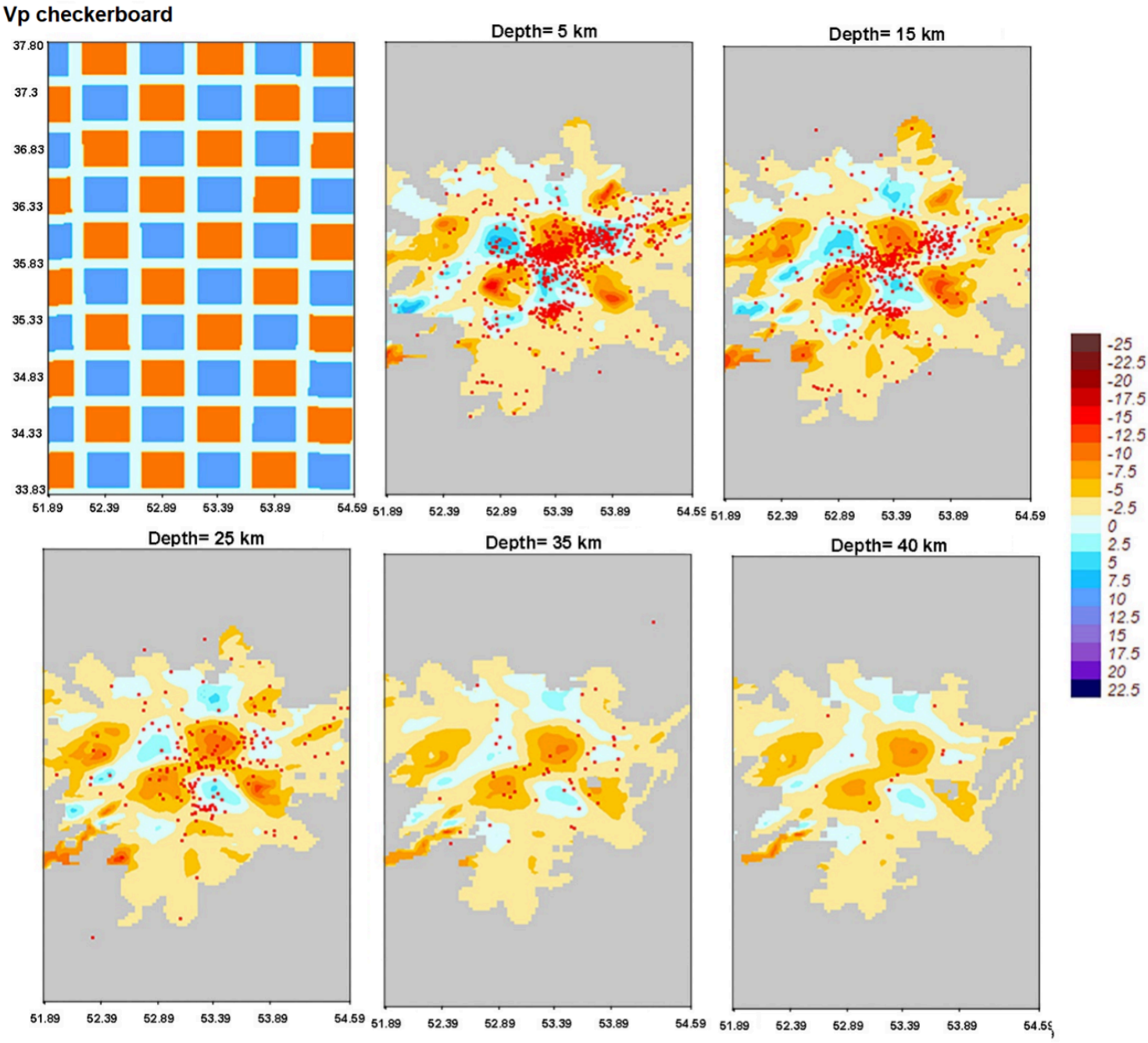


Figure 5

Checkerboard resolution test for the Vp model using the optimized inversion parameters. Recovered horizontal slices are shown at depths of 5, 15, 25, 35, and 40 km. The synthetic checkerboard model consists of alternating ±10% velocity perturbations with cell dimensions of 35 × 35 km separated by 10-km gaps.

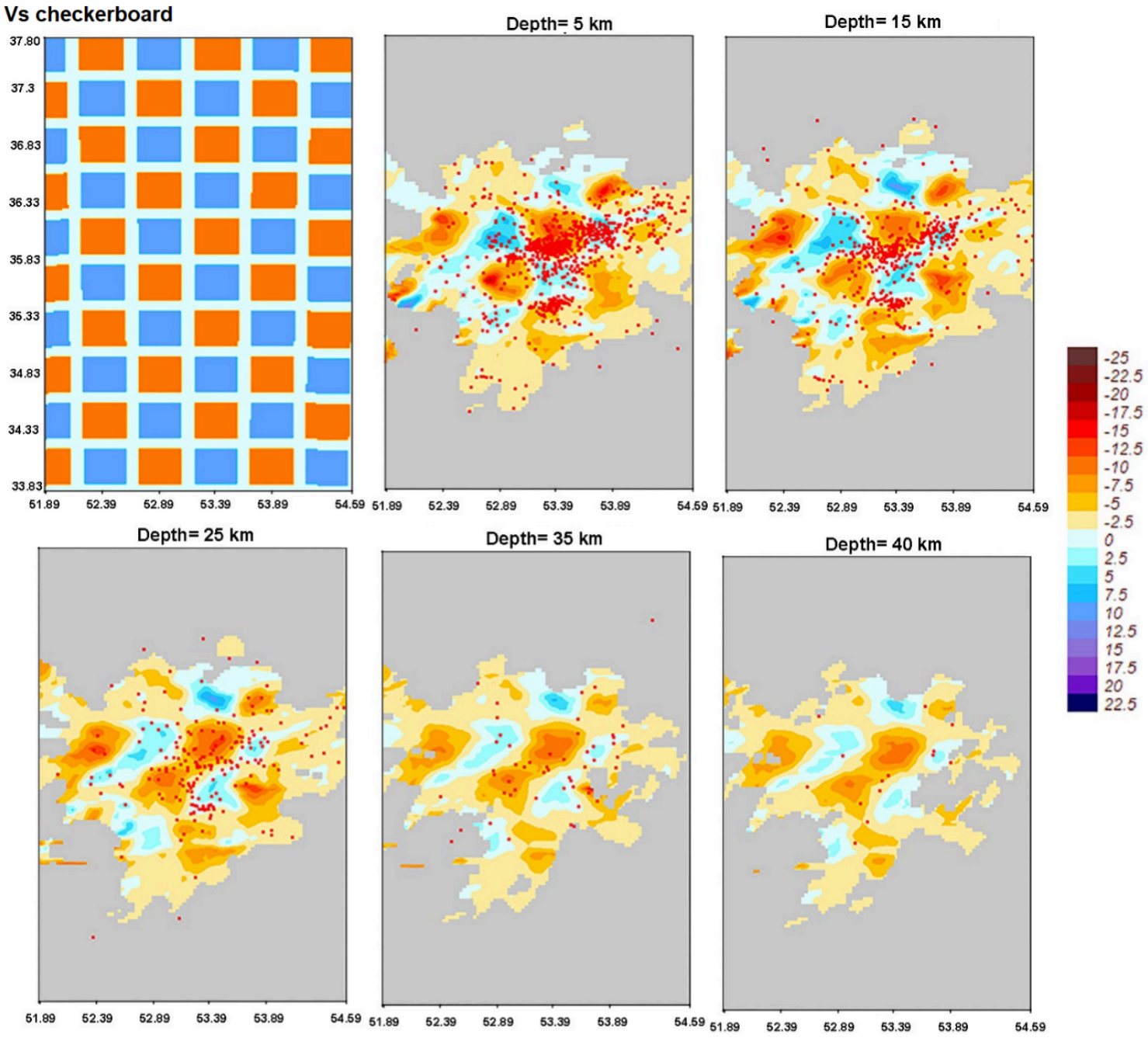


Figure 6

Checkerboard resolution test for the Vs model using the optimized inversion parameters. Recovered horizontal slices are shown at depths of 5, 15, 25, 35, and 40 km. The synthetic checkerboard model consists of alternating ±10% velocity perturbations with cell dimensions of 35 × 35 km separated by 10-km gaps.

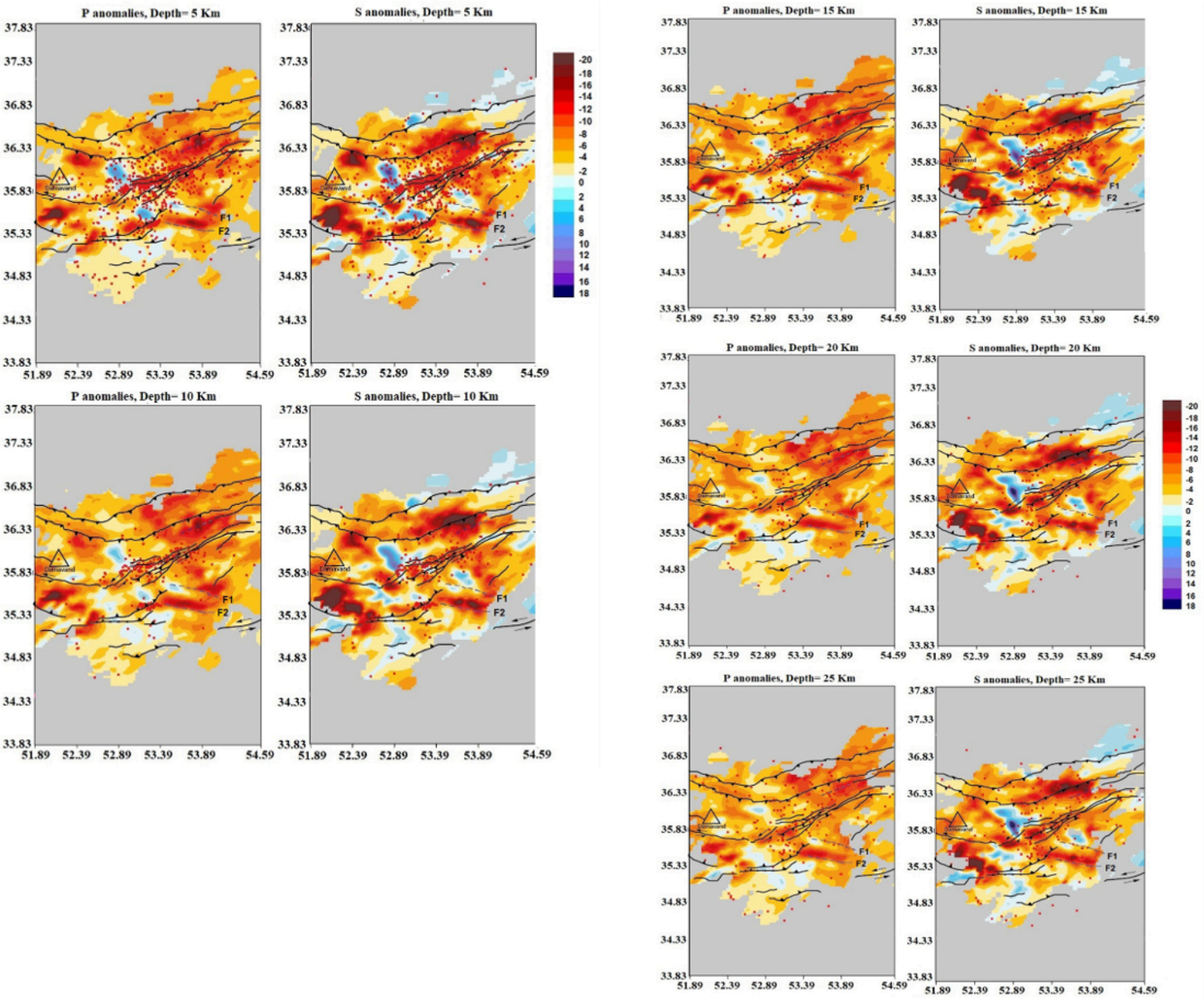


Figure 7

Three-dimensional P- and S-wave velocity tomography results derived from local earthquakes in the eastern Alborz region, together with the locations of Mount Damavand, seismic events, and mapped regional faults.

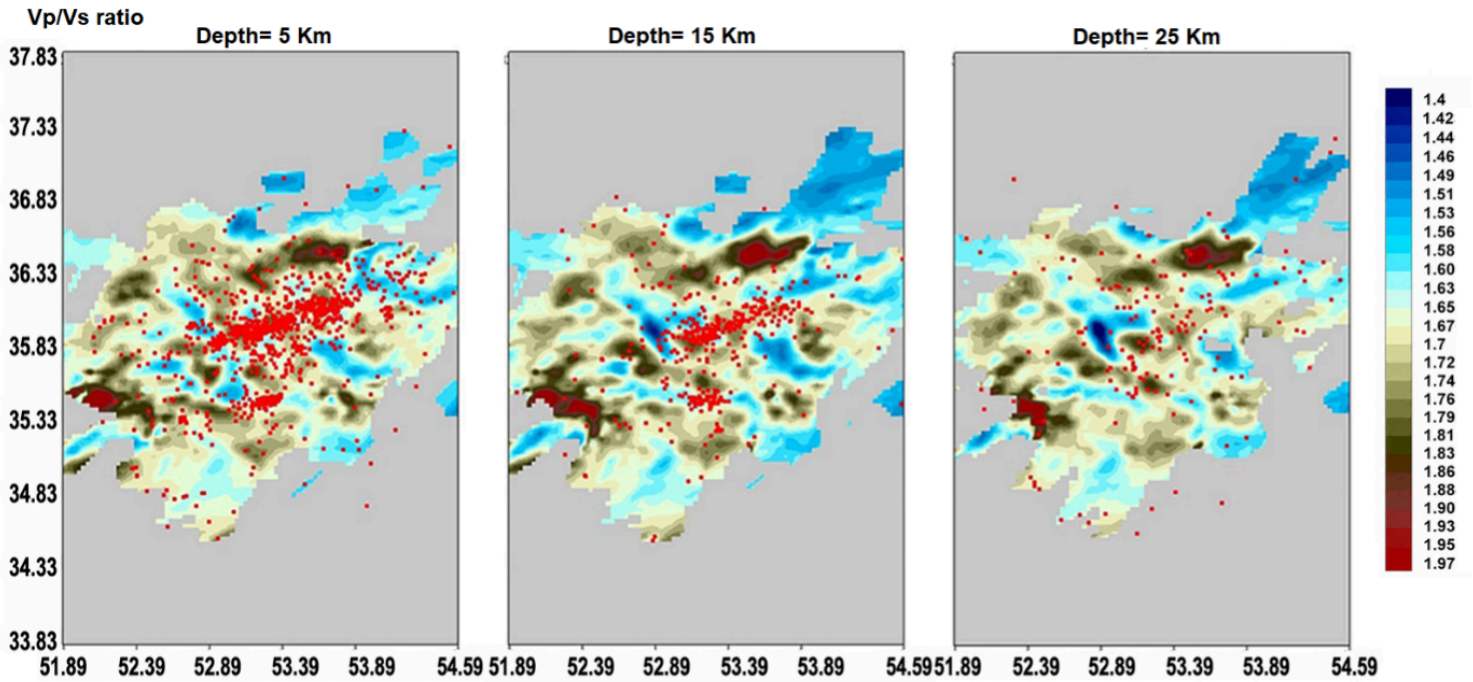


Figure 8

Horizontal slices of the Vp/Vs ratio model at depths of 5, 15, and 25 km beneath the eastern Alborz. Black lines denote mapped active faults, red circles indicate relocated earthquakes, and the triangle marks Mount Damavand.